

Strain Gauge analysis of non-axial loads in three-element implant-supported prostheses

Análise extensométrica de cargas não axiais em próteses de três elementos, implantossuportadas

Talitha de Cássia Silva SOUSA¹, Vanda de LELIS², Vivian Mayumi Miyazaki SANTOS¹, Gabriela Nogueira de Melo NISHIOKA¹, Luis Gustavo de Oliveira VASCONCELLOS¹, Renato Sussumu NISHIOKA¹

1 – Institute of Science and Technology – UNESP – Univ Estadual Paulista – School of Dentistry – Department of Dental Materials and Prosthodontics – São José dos Campos – SP – Brazil.

2 – College of Dentistry Piracicaba – UNICAMP – Univ de Campinas – Department of restorative dentistry – Piracicaba – SP – Brazil.

ABSTRACT

Objective: This study evaluated “in vitro”, the microstrain around three external hexagon implants linearly placed after static loadings on non-axial points of Co-Cr superstructures. **Methods:** The implants were inserted into a polyurethane block and their microunit prosthetic abutments were screwed with torque of 20 Ncm. Four strain gauges were linked to the block around the implants. Onto the abutments, Co-Cr superstructures (n = 5) were screwed with torque of 10 Ncm. The static vertical loads of 30 kg were applied for 10 s during 3 repetitions in four non-axial points located perpendicularly to the long axis (A and B) and another two points at the extremity of the superstructure (A' and B'). The data were recorded with the aid of a conditioner of electrical signals and the Strain-Smart software. **Results:** The results obtained were submitted to Analysis of Variance (ANOVA). **Conclusion:** It could be concluded that there were no significant differences in the effects of the applications of non-axial loads of this present study (p = 0.6464). Also, there were no differences between the displacement means, 3 mm for A and B; 5 mm for A' and B' (p = 0.8731).

KEYWORDS

Biomechanics; Dental implant; Dental prosthesis.

RESUMO

Objetivo: Este estudo avaliou, “in vitro”, as microdeformações geradas ao redor de três implantes de hexágono externo posicionados linearmente após carregamentos estáticos em pontos não axiais de supraestruturas de Co-Cr. **Métodos:** Em um bloco de poliuretano, foram inseridos os implantes e parafusados os pilares protéticos microunit com torque de 20 Ncm. Na superfície do bloco foram colados quatro extensômetros adjacentes aos implantes, sendo dois para o central. Sobre os pilares foram parafusados supraestruturas fundidas em liga de Co-Cr (n = 5) com torque de 10 Ncm. As cargas verticais estáticas de 30 kg foram aplicadas durante 10 segundos sob 3 repetições em quatro pontos não axiais localizados perpendiculares ao longo eixo (A e B) e em outros dois pontos na extremidade da supraestrutura (A' e B'). Os dados foram registrados com auxílio de um condicionador de sinais elétricos e do software Strain-Smart e os resultados obtidos foram submetidos à Análise de Variância (ANOVA) e ao teste de comparação múltipla de Tukey (5%). **Resultados:** A apresentação dos resultados foi realizada em forma gráfica e descritiva. **Conclusão:** Pode-se concluir de acordo com as análises estatísticas que não houve diferença significativa nos efeitos principais e interação do presente estudo (p = 0,6464). Nas estatísticas tabuladas não houve diferença entre as médias nos deslocamentos, 3 mm e 5 mm (p = 0,8731).

PALAVRAS-CHAVE

Biomecânica; Implantes dentários; Prótese dentária.

INTRODUCTION

The use of dental implants for oral rehabilitation of either total or partial edentulous arches has been applied to replace lost teeth, depending on the alveolar bone [1,2]. To perform these treatments, there are available in the dental market, three types of abutments, as follows: external hexagon, internal hexagon, and cone morse. External hexagon implants can be attached by a metallic bar and be used to construct a fixed partial or total prosthesis [3].

In fixed prosthesis rehabilitation, the occlusal forces are directly applied onto the prosthesis and transmitted to the bone/implant interface and the maintenance of the peri-implantar bone tissue should be the primordial fact to achieve long-term treatment success. Currently, it has been searched to reduce the biomechanical force at the bone/implant interface [4], because the increase of the mechanical stimulus may result in a bone strengthening through density and apposition, by respecting a threshold; however, mechanical stimuli above this threshold results in microdamage due to fatigue [5,6,7]. In Dentistry, varied computed-based programs can be used (such as computed guided surgeries) to evaluate the efforts of the bone structures and the statistical analysis of the clinical procedures [8]. The birefringence analysis, the strain gauge, and the bond strength studies between the implant and bone tissues, according to Spiekermann 1995, have been the main methods for biomechanical analysis and investigation. The strain gauge technique has been used to evaluate stresses in implant-supported prosthesis both in vitro [10,11], and in vivo [12,13].

Some failures of the implant system have been associated with occlusal overload as the primary factor [8,14,15,16]. As the main factor, it has been emphasized the lack of biomechanical concepts [17].

In this context, this study aimed to evaluate the microstrain of 3 implants with external hexagon abutments, placed linearly after the static loading onto non-axial points of Cobalt-Chromium superstructures simulating fixed implant-supported prostheses.

MATERIAL AND METHODS

A polyurethane block (F-16 Polyurethane Axson, Cery – France) was constructed from a silicone mold (Clássico artigos odontológicos, Catanduva-São Paulo, Brazil) and after the polishing of all surfaces with the aid of 220- to 660-grit sandpapers, a surface with a small amount of irregularities were obtained with final dimensions of: 95 mm of length x 45 mm of width x 20 mm of height .

To achieve a linear positioning of the external hexagon implants (AS Technology Titanium Fix, São José dos Campos – Brazil), an aluminum matrix was machined and composed of three components. These components were superimposed and had perforations that enabled the screwing of specific screws to achieve their union. One of these components had three central perforations with 3 mm of distance among each other which guided the block perforation and implant placement.

The component 1 (figure 1) had a rectangular base with 75 mm of length x 40 mm of width x 5 mm of thickness. In the central area, there are three cylinders 3 mm equidistant from each other. Each cylinder had 4 mm height x 4 mm diameter. In this component, there are four central perforations, bilaterally, with 2 mm of diameter enabling the screwing of specific screws to link components 2 and 3. The component 2 (figure 1) had a rectangular base with 75 mm of length x 40 mm of width x 5 mm of thickness with a central hole matching the central part of component 1. The component 3 (figure 1) had a rectangular shape with 75 mm of length, 10 mm of width and 3 mm of thickness containing 3 central orifices with 4 mm of diameter matching the location of the cylinders positioned onto the base (component 1). This last component was fixed to the block and determined the standardization of the distance and sites for the insertion of the external hexagon implants (AS Technology Titanium Fix, São José dos Campos – Brazil). Only one set of standardized and conventional burs (AS Technology Titanium Fix, São José dos Campos – Brazil) for implant installation was used: spearhead-shaped bur and helical-shaped burs of 2; 2.5; 2.8; 3.0 and 3.2 mm of diameter. The protocol for the execution of the perforations followed the conventional patterns, excluding the asepsis care. The mean speed of the



Figure 1 – (a) component (b) component 2 and (c) component 3.

perforations and the insertion was 1,800 and 14 revolutions per minute, respectively. The torque was adjusted for 40 Ncm, and the ending of the implant insertion was executed manually with the aid of the surgical ratchet wrench.

Onto the platform of implant installation, an abutment (Microunit, AS Technology Titanium Fix, São José dos Campos – Brazil) was positioned, standardized with a metallic collar of 3 mm, and screwed with 20 Ncm torque with the aid of a mechanical torquemeter (AS Technology Titanium Fix, São José dos Campos – Brazil).

By using plastic copings (AS Technology Titanium Fix, São José dos Campos, Brazil) and 5 waxings, performed and standardized through the fixation of the base of the component 1 to component 2, five superstructures were obtained (samples). This procedure enabled to reproduce systematically the waxing of all patterns. Then, the patterns were included in silicon rings by using a lining of phosphate without graphite (Bellavest SH Bego, Bremen – Germany). The casting was executed in Co-Cr alloy (Wirobond SG, Bremen - Germany) and the metal injection occurred through a conventional centrifuge. After the cooling of the samples, these were individually placed onto the prosthetic abutments, when the set stability was verified without torque and through the visual verification of the adaptation. There was no instability that determined the exclusion of the superstructure [18-19]. The four uniaxial strain gauges (KFG-02-120-C1-11N30C2 - Kyowa Electronic Instruments Co. Ltd, Tokyo – Japan) were bonded with the aid of cyanoacrylate-based adhesive (Super Bonder Loctite, São Paulo – Brazil) tangentially to the prosthetic abutments. Onto the upper extremity of the largest side of the block, the terminal plates were linked, where the electrical connections were performed.

The electrical resistance variations were transformed into microstrain units ($\mu\epsilon$) through

a conditioner of electrical signals (Model 5100B Scanner – System 5000 – Instruments Division Measurements Group, Inc. Raleigh, North Carolina – USA,) which was also responsible for recording the information. The strain-smart software installed in a computer with Pentium IV processor, 1.1 Ghz, 256 MB of RAM memory allowed the data recording. All procedure was repeated twice and the microstrain determined by the loading were registered by the four strain gauges.

After the placement of each sample onto the abutments, torque was applied starting from the central screw, followed by the left and right ones. The same hexagonal tip of 1.17 mm was adapted in a progressive torquemeter to finish the screwing with about 10 Ncm torque, following the same sequence.

To apply the load onto the samples, four non-axial points (A, A', B and B') were selected. Point A was localized at 3 mm far from the central screw of the most distal implant, towards the direction of a free surface. The point A' was 1 mm far from point A in the same direction. The point B was localized 3 mm far from the central screw of the most distal implant, towards the direction of a free surface. The point B' was 1 mm far from point B in the same direction, according to figure 2.

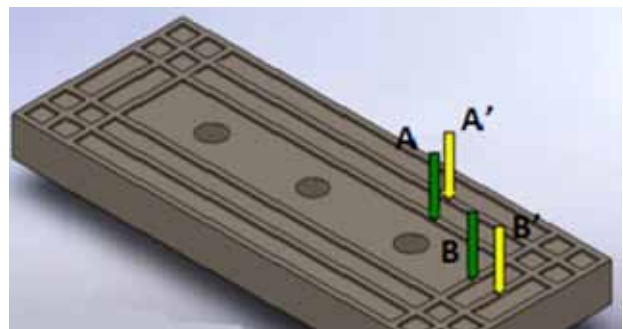


Figure 2 – The Figure illustrates the position of the points of load application. The green arrows show the points placed 3 mm far from the most distal implant (A and B). The yellow arrows show the points placed 5 mm far from the most distal implant (A' and B').

The load application was executed through a loading device. After the placement of the samples under the pressure tip, a load of 30 kg was applied for 10 s. Then the values of the 3 strain gauges were recorded. For each point, in each superstructure, 3 readings were performed and then their arithmetical mean was considered, therefore enabling a better accuracy of the measurements.

At each test of the points, the screws were retorqued and the strain gauges were reset and balanced. Data were tabulated for further assessment regarding to both the application points and the microstrain ($\mu\epsilon$) in the different areas tested.

Data were submitted to two-way ANOVA for the comparison of the means with normal distribution with level of significance of 5%.

RESULTS

In this study, the absolute microstrain were considered because the purpose was not to determine either the compressive or tensile strength of the polyurethane block. The experimental variables were the load application points and the areas where the strain gauges were linked to. The treatment means the point where the loading was performed (Table 1).

Table 1– Means of each Strain Gauge and mean of 4 Strain gauges, after the execution of the 3 loadings

Treatment	Displacement (mm)	Sample	Mean
A	3	1	37.300
A'	5	1	122.375
B	3	1	5.245
B'	5	1	1.915
A	3	2	212.163
A'	5	2	297.745
B	3	2	323.498
B'	5	2	415.747
A	3	3	99.995
A'	5	3	104.745
B	3	3	181.745
B'	5	3	251.663
A	3	4	158.413
A'	5	4	125.498
B	3	4	187.662
B'	5	4	2.913
A	3	5	135.828
A'	5	5	90.327
B	3	5	231.165
B'	5	5	109.995

Small differences were found between the sites of load application points as seen in table 1, without statistical significant differences. A microstrain pattern was not found regarding to both the linear (A to B) and centrifugal (A, A' or B, B') displacement.

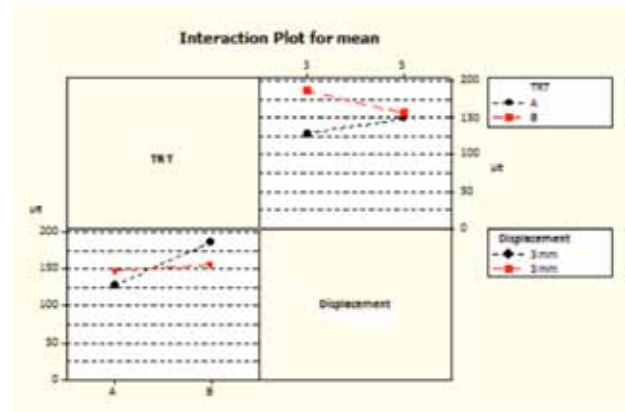


Figure 3 – Graphic of interaction of means, based on the treatments and displacements.

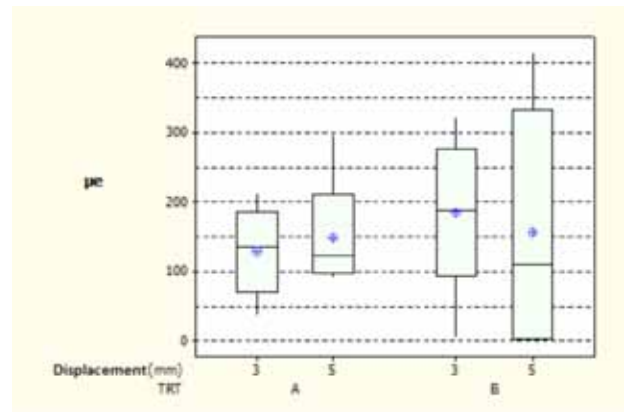


Figure 4 – Graph of the strain gauge means in each treatment (A or B) and in each displacement (A O 3 mm, A' O 5 mm and B O 3 mm and B' O 5 mm). The blue dot means the strain gauge mean.

The analysis of the points A, A', B and B', resulted in mean, median, coefficient of variation, maximum and minimum value. These results enabled to conclude that the coefficient of variation among them were similar, without statistically significant differences, despite that the maximum and minimum values are different.

Table 2– Results of the A (3 mm) and A' (5 mm) treatments, in each strain gauge (SG), and the absolute mean of the treatment**TRT Results = A and A'**

Variable	Displacement	Mean	Standard deviation	Coefficient of Variation
SG1	3	149.0	104.9	70.4
	5	208.8	149.1	71.4
SG2	3	18.26	15.03	82.32
	5	25.33	17.92	70.73
SG3	3	48.2	38.1	79.07
	5	43.6	43.1	98.82
SG4	3	299.5	178.1	59.46
	5	314.8	186.0	59.1
MEAN	3	128.7	65.3	50.75
	5	148.1	84.8	57.26

In table 3, it is observed a greater variation from treatment B to B', without statistically significant differences.

Table 3 – Results of treatments B (3 mm) and B' (5 mm), in each strain gauge (SG), and the absolute mean of the treatment**TRT Results = B and B'**

Variable	Displacement	Mean	Standard deviation	Coefficient of Variation
SG1	3	204.5	172.4	84.31
	5	173.1	205.9	118.94
SG2	3	33.1	27.1	81.78
	5	38.0	48.6	127.99
SG3	3	119.9	72.4	60.40
	5	127.7	132.1	103.46
SG4	3	386	237	61.44
	5	287	332	115.55
MEAN	3	185.9	115.8	62.3
	5	156.4	177.4	113.41

According to the strain gauges means, there were no statistically significant differences between treatment A (displacement of 3 mm) and A' (displacement of 5 mm) means, respectively 157.3 and 152.3.

According to ANOVA for repeated measurements, there were no statistically

significant differences for both the treatment ($p = 0.6464$), displacement ($p = 0.8731$) and interaction ($p = 0.4447$).

DISCUSSION

The biomechanical aspects of the osseointegrated implant are fundamentally different from those of the natural tooth, surrounding by periodontal ligament. The possibility of overload transference to the implant may exert the physiologic threshold and cause failure or even loss of the osseointegration, therefore resulting in microstrain around the implants that may hinder the long-term success of this rehabilitative treatment [11,20,21].

The highest successful rates of implants have been observed in areas with bone tissue type D1 and D2 of Zarb's classification [16]; however, in predominantly bone marrow these results have seemed to be not very satisfactory [22,23]. In this context, the study object with the same modulus of elasticity of bone marrow (polyurethane = 3.6 GPa and bone marrow = 4.25 GPa) provides an acceptable simulation of the clinical practice. Other authors also used this artificial model considering that it shows uniform elastic characteristics [24,25]; however, the literature also reports studies employing bone blocks [12,13,26,27].

External hexagon implants were chosen because they have been considered as the least stable when compared with internal hexagon implants [28,29] and they possibly provide greater microstrain at the peri-implantar area. Notwithstanding, Nishioka et al. 2011 showed that these differences were not statistically significant in a study conducted similarly to this present study. However, it is possible to find in the literature studies verifying that the connection type is relevant for the microstrain around the implants [31], but differently from this study, the finite element analysis was performed with single crowns.

The choice for the linear positioning of the implants followed the line of reasoning

of Nishioka et al. 2011 who did not find statistically significant differences between this linear and offset position. Concerning to the linear positioning of the strain gauges, this study is in agreement of the study conducted by Heckmann et al., 2004, among others, who studied the microstrain around the implants with 3-element superstructures [30,32-38]. This position justifies the little variation found in the microstrain means of the non-axial loads executed by this present study, and the highest values were found in the points farthest from the implant e (A' and B'). This affirmation can be justified by the study of Cehreli et al. 2004 who affirmed that the positioning of the strain gauges influenced on the results of the types of the microstrain found.

The load of 30 kg employed in this study is based on the study of Mericske-Stern et al. (1995) who found values close to those found in this present study in the recordings of masticatory load in vivo, and it is in agreement with other studies of masticatory load [40].

The use of superstructures in implant-supported prostheses casted in Co-Cr alloy is equally acceptable to the employment of Pd-Ag alloy because of its low cost, biocompatibility and durability so that it was the alloy type chosen by this present study [41].

Other important characteristic observed was that the microstrain means stayed inside the bone threshold of physiologic microstrain proposed in literature [5,7].

CONCLUSION

Based on the results obtained with the methodology employed, it can be concluded that the points of load application – non-axial and perpendicular to the long axis (A and B) and other two points at the extremity of the superstructure (A` and B`) did not statistically interfered on the magnitude of the microstrain of the surfaces analyzed. Also, the tensions generated in the areas studied stayed within the physiologic thresholds regardless of the axiality of the loads.

REFERENCES

1. Branemark PI. Introduction to osseointegration. In: Branemark PI, Zarb GA, Albrektsson T, editors. *Tissueintegrated prostheses: osseointegration in clinical dentistry*. Chicago: Quintessence Publ; 1985. p. 11-76.
2. Lavstedt S, Bolin A, Henrikson CO. Proximal alveolar bone loss in a longitudinal radiographic investigation. II. A 10-year follow-up study of an epidemiologic material. *Acta Odontol Scand*. 1986;44(4):199-205.
3. Branemark PI. Osseointegration and its experimental background. *J Prosthet Dent*. 1983;50(3):149-60.
4. Çehreli M, Sahin S, Akça K. Role of mechanical environment and implant design on bone tissue differentiation: current knowledge and future contexts. *J Dent*. 2004;32(2):123-32.
5. Frost HM. Wolff's Law and bone's structural adaptations to mechanical usage: an overview for clinicians. *Angle Orthod*. 1994;64(3):175-88.
6. Isidor F. Influence of forces on peri-implant bone. *Clin Oral Implants Res*. 2006; 17 Suppl 2:8-18.
7. Wiskott HW, Belser UC. Lack of integration of smooth titanium surfaces: a working hypothesis based on strains generated in the surrounding bone. *Clin Oral Implants Res*. 1999 Dec;10(6):429-44.
8. Naert I, Quirynen M, Van Steenberghe D, Darius P. A study of 589 consecutive implants supporting complete fixed prostheses. Part II: Prosthetic aspects. *J Prosthet Dent*. 1992;69(6):949-56.
9. Spiekermann H, Donath K, Hassel TM, Jovanovic S, Richter EJ. *Biomechanics. Color atlas of dental medicine implantology*. In: __ *Biomechanics*. New York: Thieme Medical Publishers; 1995. p. 81-90.
10. Assif D, Marshak B, Horowitz A. Analysis of load transfer and stress distribution by an implant-supported fixed partial denture. *J Prosthet Dent*. 1996;3(3):285-91.
11. Clelland NL, Gilat A, McGlumphy EA, Brantley WA. A photoelastic and strain gauge analysis of angled abutments for an implant system. *Int J Oral Maxillofac Implants*. 1993;8(5):541-8.
12. Cehreli M, Duyck J, De Cooman M, Puers R, Naert I. Implant design and interface force transfer. A photoelastic and strain-gauge analysis. *Clin Oral Implants Res*. 2004 Apr;15(2):249-57.
13. Duyck J, Ronald HJ, Van Oosterwyck H, Naert I, Vander Sloten J, Ellingsen JE. The influence of static and dynamic loading on marginal bone reactions around osseointegrated implants: an animal experimental study. *Clin Oral Implants Res*. 2001 Jun;12(3):207-18.
14. Adell R, Lekholm U, Rockler B, Branemark PI. A 15-year study of osseointegrated implants in the treatment of the edentulous jaw. *Int J Oral Surg* 1981;10(6):387-416.
15. Isidor F. Loss of osseointegration caused by occlusal load of oral implants. A clinical and radiographic study in monkeys. *Clin Oral Impl Res* 1996;7(2):143-52.
16. Zarb GA, Schmitt A. The longitudinal clinical effectiveness of osseointegrated dental implants: The Toronto study. Part III: Problems and complications encountered. *J Prosthet Dent*. 1990;64(2):185-94.
17. Jansen VK, Conrads G, Richter EJ. Microbial leakage and marginal fit of the implant-abutment interface. *Int J Oral Maxillofac Impl*. 1997;12(4):527-40. Publ; 1985. p. 11-76.

18. Byrne D, Houston F, Cleary R, Claffey N. The fit of cast and premachined implant abutment. *J Prosthet Dent.* 1998;80(2):184-92. Branemark PI. Osseointegration and its experimental background. *J Prosthet Dent.* 1983;50(3):149-60.
19. Carr AB, Brunski JB, Hurley E. Effects of fabrication, finishing and polishing procedures on preload in prostheses using conventional "gold" and plastic cylinders. *Int J Oral Maxillofac Implants.* 1996;11(5):589-98.
20. Assunção WG, Barão VA, Tabata LF, Gomes EA, Delben JA, dos Santos PH. Biomechanics studies in dentistry: bioengineering applied in oral implantology. *J Craniofac Surg.* 2009 Jul;20(4):1173-7.
21. Eskitascioglu G, Usumez A, Sevimay M, Soykan E, Unsal E. The influence of occlusal loading location on stresses transferred to implant-supported prostheses and supporting bone: A three-dimensional finite element study. *J Prosthet Dent.* 2004 Feb;91(2):144-50.
22. Jaffin RA, Berman CL. The excessive loss of Branemark fixtures in type IV bone: a 5-year analysis. *J Periodontol.* 1991 Jan;62(1):2-4.
23. Rangert B, Krogh PH, Langer B, Van Roekel N. Bending overload and implant fracture: a retrospective clinical analysis. *Int J Oral Maxillofac Implants.* 1995 May-Jun;10(3):326-34.
24. Watanabe F, Uno I, Hata Y, Neuendorff G, Kirsch A. Analysis of stress distribution in a screw-retained implant prosthesis. *Int J Oral Maxillofac Implants.* 2000 Mar-Apr;15(2):209-18.
25. Heckmann SM, Karl M, Wichmann MG, Winter W, Graef F, Taylor TD. Cement fixation and screw retention: parameters of passive fit. An in vitro study of three-unit implant-supported fixed partial dentures. *Clin Oral Implants Res.* 2004 Aug;15(4):466-73.
26. Çehreli MC, Akkocaoglu M, Comert A, Tekdemir I, Akca K. Human ex vivo bone tissue strains around natural teeth vs. immediate oral implants. *Clin Oral Implants Res.* 2005 Oct;16(5):540-8.
27. Akça K, Kokat AM, Sahin S, Iplikçioğlu H, Çehreli MC. Effects of prosthesis design and impression techniques on human cortical bone strain around oral implants under load. *Med Eng Phys.* 2009;31(7):758-63.
28. Park JK, Choi JU, Jeon YC, Choi KS, Jeong CM. Effects of abutment screw coating on implant preload. *J Prosthodont.* 2010 Aug;19(6):458-64.
29. Bernardes SR, de Araujo CA, Neto AJ, Simamoto Junior P, das Neves FD. Photoelastic analysis of stress patterns from different implant-abutment interfaces. *Int J Oral Maxillofac Implants.* 2009 Sep-Oct;24(5):781-9.
30. Nishioka RS, de Vasconcellos LG, de Melo Nishioka GN. Comparative strain gauge analysis of external and internal hexagon, Morse taper, and influence of straight and offset implant configuration. *Implant Dent.* 2011 Apr;20(2):e24-32.
31. Chun HJ, Shin HS, Han CH, Lee SH. Influence of implant abutment type on stress distribution in bone under various loading conditions using finite element analysis. *Int J Oral Maxillofac Implants.* 2006 Mar-Apr;21(2):195-202.
32. Nishioka RS, Nishioka LN, Abreu CW, de Vasconcellos LG, Balducci I. Machined and plastic copings in three-element prostheses with different types of implant-abutment joints: a strain gauge comparative analysis. *J Appl Oral Sci.* 2010 Jun;18(3):225-30.
33. Nishioka RS, Vasconcellos LGO, Nishioka LNBM. External Hexagon and Internal Hexagon in Straight and Offset Implant Placement: Strain Gauge Analysis. *Implant Dent.* 2009;18(6):512-20. Assunção WG, Barão VA, Tabata LF, Gomes EA, Delben JA, dos Santos PH. Biomechanics studies in dentistry: bioengineering applied in oral implantology. *J Craniofac Surg.* 2009 Jul;20(4):1173-7.
34. Abreu CW, Vasconcellos LGO, Balducci I, Nishioka RS. A comparative study of microstrain around three-morse taper implants with machined and plastic copings under axial loading. *Braz J Oral Sci.* 2010 Jan-Mar;9(1): 11-5.
35. Nishioka RS, Santos VMM, Nishioka GNM, Balducci I. A comparative study of microstrain around three-morse taper implants, casting with machined and plastic copings, under axial loading. *Rev Odontol UNESP.* 2011 Jan-Feb;41(1):56-61.
36. Vasconcellos LGO, Nishioka RS, Vasconcellos LMR, Nishioka LNBM. Effect of axial loads on implant-supported partial fixed prostheses by strain gauge analysis. *J Appl Oral Sci.* 2011;19(6):610-5.
37. Abreu CW, Nishioka RS, Balducci I, Consani LX. Straight and offset implant placement under axial and nonaxial loads in implant-supported prostheses strain gauge analysis. *J Prosthodont.* 2012; Oct;21(7):535-9. doi: 10.1111/j.1532-849X.2012.00871.x.
38. Santos VMM, Sousa TCS, Louzada FF, Nishioka GNM, Nishioka RS. Strain Gauge: study of strain distributions around three Morse taper prosthetic connections with offset positioning in machined and plastic copings under vertical load. *Braz Dental Sci.* 2012;15(3):50-5.
39. Mericske-Stern R, Assal P, Mericske E, Burgin W. Occlusal force and oral tactile sensibility measured in partially edentulous patients with ITI implants. *Int J Oral Maxillofac Implants.* 1995 May-Jun;10(3):345-53.
40. Kogawa EM, Calderon PS, Lauris JR, Araújo CR, Conti PC. Evaluation of maximal bite force in temporomandibular disorders patients. *J Oral Rehabil.* 2006;33(8):559-65.
41. Hollweg H, Jacques L, Moura M, Bianco V, Sousa E, Rubo J. Deformation of implant abutments after framework connection - a study with strain gauges. *J Oral Implantol.* 2010 Jul 21. [Epub ahead of print]

Talitha de Cássia Silva Sousa
(Corresponding address)

Departamento de Materiais Odontológicos e Prótese -
Faculdade de Odontologia de São José dos Campos, UNESP
Av. Francisco José Longo, 777 - São José dos Campos
CEP: 12245-000
Fone: (11) 3622-5917
E-mail address: talitha.sousa@fosjc.unesp.br

Date submitted: 2013 Feb 14

Accept Submission: 2013 Mai 13